

EMITTANCE MEASUREMENT BY USING DUO IMAGE PATTERN OF CHERENKOV RADIATION*

Jiaer Chen, Anjia Gu, Rongli Geng, Yuantao Ding, Kui Zhao, Baocheng Zhang, Shengwen Quan
RFSC Group, Institute of Heavy Ion Physics, Peking University, Beijing 100871, P.R. China

Abstract

The emittance of the electron beam is to be measured by using Cherenkov radiation in a novel way. The image patterns of the radiation are formed both in the focal plane and image plane of an achromatic lens with long focus. Both the angular spread and radial distribution of the e-beam are obtained by processing both patterns and in this way the beam RMS emittance is directly resulted. Combining this technology with computerized tomography (CT), the actual particle density distribution in transverse phase space can be determined without any pre-assumptions. The emittance of the electron beam from the DC-SC photo-injector of Peking University is simulated and a He-Ne laser experiment is presented and discussed in this paper.

1. INTRODUCTION

For the conventional optical diagnostics using Cherenkov Radiation (CR) or Optical Transition Radiation (OTR), quadrupole-scanning techniques or “tri-gradient method” are often used to determine the e-beam emittance indirectly. The assumption of an elliptical contour in the beam phase space actually brings systematic errors.

According to parameters of the DC-SC photo-injector at Peking University^[1], the energy of the e-beam is 2-3 MeV. OTR at this level is too weak to be captured by a CCD camera. In this paper a new direct way of emittance measurement by using Duo Image Pattern of Cherenkov Radiation is introduced, which can measure the angular spread and the radial distribution of the electron beam simultaneously. Combining this method with CT, a complete phase space tomography can be made without any assumptions on the distribution of e-beam phase space and the extrapolation of angles in Radon transformation.

2. RMS EMITTANCE MEASUREMENT

As a charged particle travelling at velocity v through a dielectric medium (refractive index n), CR is emitted in a thin cone centered on the trajectory with opening angle θ_c , when $v > C/n$. In Fig. 1, θ_c , θ_i , θ_r , θ_t and θ_f are angles corresponding to Cherenkov angle, internal incident angle, external refracted angle, tilted angle of the converter, and observation angle, respectively.

Using Snell’s law, the observation angle:

$$\theta_f = \arcsin(n \sin(\theta_c - \theta_i)) \approx n(\theta_c - \theta_i)$$

where, $\theta_c = \arccos(1/\beta n)$, the CR angle.

Suppose r'_i is the divergence angle of the i^{th} particle in the beam as it passes through the converter, then:

$$\theta_{f_i} = \arcsin(n \sin(r'_i + \theta_{c_i} - \theta_{i_i})) = \arcsin(n \sin r'_i)$$

Setting $\theta_f = \theta_c$ approximately $\theta_f \approx nr'_i$.

Hence, the one-to-one correspondence between the observation angle of CR and the divergence angle of the e-beam is derived. According to this correspondence, Sandia Lab. devised an array of mirrors to split the CR into six different angular slices. In order to obtain an angular resolution of a few mrad, the cameras must be placed at a distance of 30m away from the Cherenkov converter^[3].

In fact, by utilization of Fourier Transform and optical imaging technique, the information of angular spread can be obtained directly from the pattern on focal plane of the lens. For this purpose, an achromatic lens with long focus is added normally to the direction of observation (Z-axis) (as in Fig.2), and it can be shown, $y_f = f \tan \theta_f$, with small angle approximation, $y_f \approx f \theta_f = f \cdot n \cdot r'_i$, where y_f is the vertical ordinate on the focal plane of the lens, f is the focus of the lens.

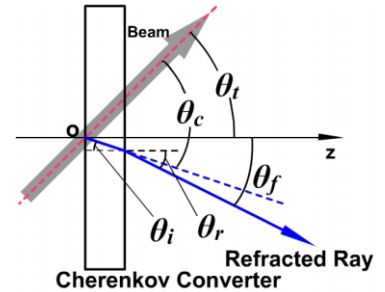


Fig.1. The angle relationship of CR

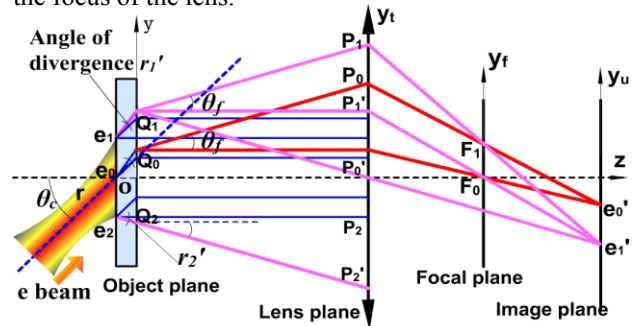


Fig.2. The optical path of “Duo Image Pattern of CR”

In principle this process can be called as “Duo Image Pattern”: while the radial distribution of the e-beam is attained from the image plane of the lens (as is widely acknowledged in the conventional optical diagnostics), the additional information of the angular spread of the e-beam is obtained from the focal plane of the lens at the same time. Consequently, we can work out $\langle y \rangle$ and $\langle y' \rangle$ from these two distributions by using statistics. According to the definition, the RMS emittance can be expressed directly as^[4].

* Supported by NSFC (10075006, 19985001)

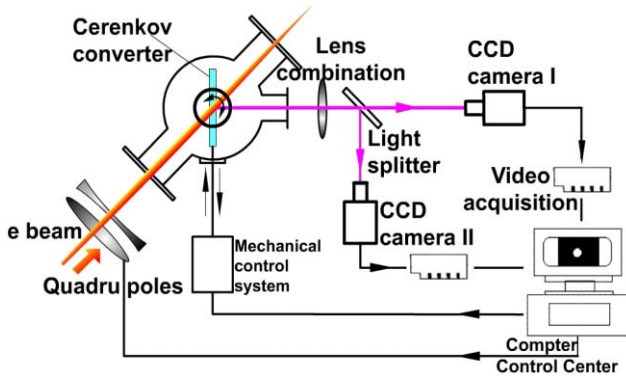


Fig.3. The Schematic view of "Duo Image Pattern" beam diagnostics of PKU-SCAF DC-SC photo injector

$$\varepsilon_{RMS} = 4 \left[\langle (y - \langle y \rangle)^2 \rangle \langle (y' - \langle y' \rangle)^2 \rangle - \langle (y - \langle y \rangle)(y' - \langle y' \rangle) \rangle^2 \right]^{1/2}$$

Fig.3 shows the layout of "Duo Image Pattern" beam diagnostics of the DC-SC photo-injector. Passing the combining lens, the CR is split by a light splitter. CCD cameras are placed at each branch of light, where locates the focal and image planes of the lens respectively.

Through simulation experiments, the errors derived from small angle approximation and image processing are rather low (less than 5%); yet the energy divergence of the beam takes a major part. An energy divergence of 2% at 3 MeV results in $\theta_c < 0.04\%$; while 30 MeV results in $\theta_c < 0.0007\%$. This method prefers e-beams of higher energy.

3. BEAM PHASE SPACE TOMOGRAPHY

3.1. The Difficulties in the Conventional Phase Space Tomography

CT refers to the cross-sectional imaging of an object from transmission data collected by illuminating the object from many different directions.

An object is represented by a two-dimensional function $f(x, y)$; the Radon transform of $f(x, y)$ is the line integral of f parallel to axis y_1 as illustrated in Fig.4:

$$p(x_1, \theta) = \int_{-\infty}^{\infty} f(x_1, y_1) dy_1$$

$$= \int_{-\infty}^{\infty} f(x \cos \theta + y \sin \theta, x \sin \theta - y \cos \theta) dy, \theta \in [0, \pi)$$

The deficiency of rotation angle

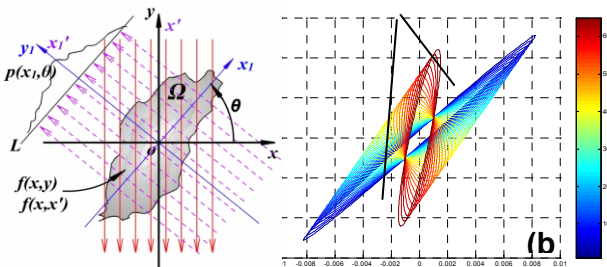


Fig.4. a. CT principles: rotation of a CT machine; b. The angle deficiency in rotation of phase-space distribution by

Changing the two-dimensional function $f(x, y)$ to $f(x, x')$, defined as the distribution function of beam phase space density, it is found that if the phase space could be rotated without distortion freely from 0 to π by some

certain transferring devices, then the CT principle can be fully applied into phase space reconstruction because of the similarity between them.

Practically, quadrupoles are used to twist the phase space^[5]. However, the whole effect includes both rotation and distortion. In addition, a considerable amount of Radon rotation angle is unavailable (shown in Fig.4). By algebra deduction and combination with CT, "Duo Image Pattern" can overcome these two difficulties successfully.

Firstly, the effect of quadrupole-scanning can be decomposed into two parts: rotation and distortion.

The transfer matrix M (consisted of quadrupole section and drift sections) is:

$$M_{BA} = \begin{pmatrix} m_{11} & m_{12} \\ m_{21} & m_{22} \end{pmatrix} = \begin{pmatrix} p_a \cos \theta_1 & p_a \sin \theta_1 \\ p_b \sin \theta_2 & p_b \cos \theta_2 \end{pmatrix}$$

$$= \begin{pmatrix} \frac{p_a}{\sqrt{p_a^2 p_b^2 - 1}} & 0 \\ \frac{1}{p_a} & \frac{1}{p_a} \end{pmatrix} \begin{pmatrix} \cos \theta_1 & \sin \theta_1 \\ -\sin \theta_1 & \cos \theta_1 \end{pmatrix} = M_A M_R \quad (3)$$

$$\text{Where } p_a = \sqrt{m_{11}^2 + m_{12}^2}, \theta_1 = \arctan \frac{m_{12}}{m_{11}} \quad (4)$$

M_A is the affined transform matrix and M_R is the unit rotation matrix. Thus, we decompose the whole effect of quadrupole-scanning into two parts, i.e. the affined transform matrix and the unit rotation matrix, corresponding to distortion and pure rotation respectively. The affined transform results in a scaling of p_a in phase space projection over horizontal ordinate. In this way, a clearer understanding between the CT principle and phase space tomography is established.

Secondly, putting the quadrupole settings and drift section into the Eq.3,4, we find that the range of θ_1 (Radon angle) cannot cover $0-\pi$ by all means^[6]. As shown in Fig.4b, there exists considerable deficiency of Radon rotation angle, no matter how many quadrupoles are adopted. By strictly choosing the parameters of the quadrupoles settings and drift sections, Duke University FEL Laboratory (DFELL) once attained the range of θ from 0 to 0.96π , still leaving a deficiency of 7° ^[5].

Since a full π radian of the rotation angle is the basic requirement of Radon transforms, in order to extrapolate the data for this deficiency, prior assumption about phase space distribution has to be made. That yields errors in the reconstructed phase space.

3.2. Applying "Duo Image Pattern" in Phase Space Tomography

By means of "Duo Image Pattern", we obtained the angular spread and radial distribution of the e-beam simultaneously^[2], as shown in Fig.5. According to the similarity between Radon Transform and the rotation of beam phase space distribution discussed above, the Radon projection of the angular spread indicates the line integral of $\int_{-\infty}^{\infty} f(x, x') dx$. As to the algorithm of CT image reconstruction, this integral is equal to $\int_{-\infty}^{\infty} f(x, x') dx'$, the Radon projection of the radial distribution of e-beam.

By applying Duo Image Pattern in the phase space tomography, both of the integrals are practicable. When a deficiency appears in Radon projection of the radial distribution on the image plane of the lens, the data from the projection of the angular spread (i.e. from the pattern on the focal plane of the lens) can be used for compensation, with some linear algebra transform in advance^[6]. Therefore, a complete phase space tomography is feasible, by putting the additional information of the angular spread in the Radon Transform (shown in Fig.5).

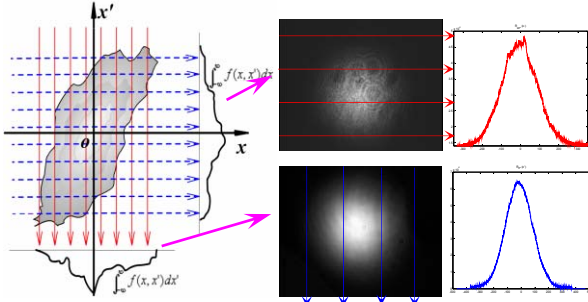


Fig.5. Phase-space tomography for the angular spread and the radial distribution by using “Duo Image Pattern”.

4. SIMULATION EXPERIMENTS

4.1. Simulation Experiment with He-Ne Laser

A He-Ne Laser is used to perform the simulation experiment so as to test the Duo Image Pattern principles. The images at the focal plane and the image plane are illustrated by Fig.6a, b, respectively. Fig.6 c, d present the 3D plot of the distribution and e, f present the profiles along the centerline of a, b. The program works out:

$$\langle x \rangle = \sum x_i p_i, \sigma = (\sum [x_i - \langle x \rangle]^2 p_i)^{1/2}, \text{ yielding:}$$

| $\langle x \rangle$ (mm) | σ_x (mm) | $\langle x' \rangle$ (mrad) | $\sigma_{x'}$ (mrad) | $\langle (x - \langle x \rangle)^* (x' - \langle x' \rangle) \rangle$ (mrad) | ϵ_{rms} (π mm mrad) | $\Delta\epsilon$ % |
|-----------------------------|--------------------|--------------------------------|-------------------------|---|--------------------------------------|-----------------------|
| 0.793 | 0.214 | 2.702 | 0.705 | 0.075 | 0.525 | 4.76 |

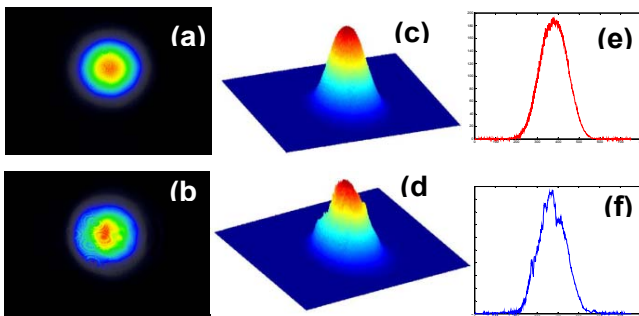


Fig.6. Simulation with He-Ne Laser and the image processing.

Via “Tri-profile Method”, the emittance of the He-Ne laser results in 0.5 π mmrad. The difference in percentage between these two methods is around 5%.

4.2. Computer Simulation of Phase-space Tomography

In order to test Duo Image Pattern algorithm in beam phase space tomography, we used a computer model to simulate the measurement and reconstruction process.

First we create an initial phase space distribution in the shape of an asymmetric combined ellipse (Fig.7.a,b), considering the actual phase space distribution generally would be irregular and non-uniform. Then, the simulation transports the distribution through the initial drift section, the combined quadrupoles and the final drift section. The program generates series of images at the focal plane and the image plane of the lens respectively, and calculates the beam’s spatial projection with rotation angle from 0° to 90° by integrating the final distribution over its angular spread and from 90° to 180° over its radial distribution^[6]. The process of the transform and the final reconstructed phase space are shown as Fig.7 c, d, presenting the high quality in this reconstruction.

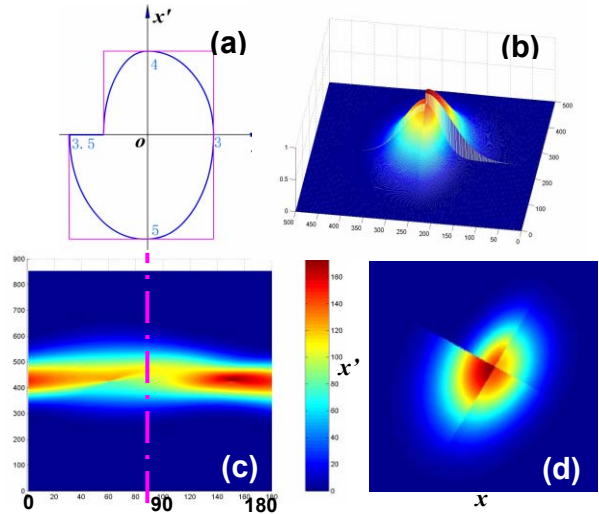


Fig.7. Phase space distribution reconstruction (colour)
a. An assumed model; b. The original distribution of the model; c. The process of Radon Transform;
d. The reconstructed phase space distribution.

5. CONCLUSION

All the simulation experiments show that “Duo Image Pattern of Cherenkov Radiation” is more useful for direct measurement of e-beam RMS emittance and for more complete tomography of phase space distribution, since it can provide additional information missed by other methods and can thus realize a full π radian Radon Transform.

6. REFERENCES

- [1] Zhao Kui, Hao Jiankui, Hu Yanle, et al. Nucl. Instr. & Meth. In Phys. Res., 2001, A475:564-568
- [2] GU An-Jia, DING Yuan-Tao, ZHAO Kui, et al. HEP & NP, 2003, 27(2):163-168 (in Chinese)
- [3] Richardson R.D., Platt R.C., Crist C.E.. Particle Accelerator Conference, 1993, vol.3: 2456 -2458
- [4] Stanley Humphries, Jr., Charged Particle Beams. Translated Chinese Edition: Beijing, 1999:57
- [5] McKee C B, O’Shea P G, et al. Nucl. Instr. & Meth. In Phys. Res., 1995, A358:264-267
- [6] GU An-Jia, ZHAO Kui, DING Yuan-Tao, et al. HEP & NP, 2003, 27(5):455-459 (in Chinese)